Liquid Crystals
Publication details, including instructions for authors and subscription information:
http://www.informaworld.com/smpp/title~content=t713926090

Side chain liquid crystalline diethanolamine-based polyesters with methoxy and/or nitroazobenzene mesogenic moieties

M. Huskić[a]; M. Žigon[a]
[a] National Institute of Chemistry, 1001 Ljubljana, Slovenia

To cite this Article Huskić, M. and Žigon, M.(2006) 'Side chain liquid crystalline diethanolamine-based polyesters with methoxy and/or nitroazobenzene mesogenic moieties', Liquid Crystals, 33: 8, 883 — 890
To link to this Article: DOI: 10.1080/02678290600884039
URL: http://dx.doi.org/10.1080/02678290600884039

Liquid Crystals, Vol. 33, No. 8, August 2006, 883–890

Side chain liquid crystalline diethanolamine-based polyesters with methoxy and/or nitroazobenzene mesogenic moieties

M. HUSKIĆ* and M. ŽIGON
National Institute of Chemistry, POB 660, 1001 Ljubljana, Slovenia

(*Received 22 August 2005; in final form 22 May 2006; accepted 26 May 2006*)

Side-chain polyesters based on diethanolamine and 5-hydroxyisophthalic acid with mesogenic methoxyazobenzene and nitroazobenzene groups were synthesized and their liquid crystalline properties were examined.

Four different types of polyesters were prepared by using various combinations of monomers differing in the mesogen group and the length of the spacer. The thermal and structural properties depend on the type of polyester as well as on the side chain length. The glass transition and isotropization temperatures increase when the methoxyazobenzene group is bound to a diol and decrease when it is bound to an isophthalic acid. Most of the polyesters are thermotropic liquid crystals and form a nematic phase on heating. Some polyesters exhibit shear induced isotropisation to nematic transition up to 25°C above the isotropization temperature.

1. Introduction

Side chain liquid crystalline (SCLC) polymers have received increasing attention due to their potential applications in the field of nonlinear optics, ferroelectrics, and optoelectronics [1–5]. Since polymers with photochromic azobenzene moieties in the side chain are promising materials for reversible data storage and nonlinear optical applications, much of the literature deals with the synthesis and properties of this type of polymer. The polymers investigated are mostly based on polyacrylates or polymethacrylates [6–8], polysulphones [9], polystyrene [10, 11] and polyesters [12–15]. The SCLC polyesters are particularly interesting as the main chain can be tailored to particular specifications by using different acidic and diol segments, both of which provide the linking unit for the various mesogenic groups. Accordingly, SCLC polyesters were synthesized with the mesogenic group bonded to either an acid [12, 15] or diol [13] or both [14, 16].

Liquid crystalline diols based on bis(2-hydroxyethyl)amine have already been proven to induce liquid crystalline properties in polyurethanes [17, 18]. Polyesters have also been synthesized; some of these were liquid crystals [19] but most formed a crystal smectic phase [20, 21].

The aim of our work was to investigate the LC properties of SCLC polyesters with diazobenzene mesogenic groups bound to diol and aromatic isophthalic acid, with variation of the type of mesogenic group as well as the spacer length. Most of the polyesters with a mesogenic group on diol and acid reported in literature were only aliphatic, polymalonates [14, 16]. Methoxyazobenzene (M) or nitroazobenzene (NO) groups were bound via a hexamethylene spacer to dimethyl 5-hydroxyisophthalate (IM6 and INO6, respectively) and via a hexa-, octa- or deca-methylene spacer to diethanolamine (M*n*-diol and NO*n*-diol respectively; $n=6$, 8, 10, the number of methylene units in the spacer). The polyesters were synthesized by *trans*-esterification and characterized by NMR spectroscopy, differential scanning calorimetry (DSC), size exclusion chromatography (SEC) polarizing optical microscopy (POM), and X-ray diffraction (XRD). The influences on LC properties by the side chain length of the diol, as well as the type of mesogenic unit used, are discussed. Additionally, for some polyesters a shear-induced isotropic–nematic transition was observed. Such a transition has only been observed in a few thermotropic [22–24] and liotropic LC polymers [25]. Although this is a rare phenomenon it is the subject of extensive research especially in rheology [26–28]

2. Experimental

2.1. *Synthesis*

The synthesis of M*n*-diol and NO*n*-diol is described elsewhere, since they have already been used as diols in

---

*Corresponding author. Email: miro.huskic@ki.si

Liquid Crystals
ISSN 0267-8292 print/ISSN 1366-5855 online © 2006 Taylor & Francis
http://www.tandf.co.uk/journals
DOI: 10.1080/02678290600884039

the synthesis of LC polyurethanes [17, 18] The synthetic procedure for IM6 and INO6 is shown in scheme 1. The first step is the synthesis of dimethyl 5-hydroxyisophthalate, which is described elsewhere [29]. 1-Bromo-6-(4-nitroazobenzene-4′-oxy)hexane and 1-bromo-6-(4-methoxyazobenzene-4′-oxy)hexane were synthesized according to the method described by Crivello [30].

In the polymerization procese 1 g of IM6 or INO6 and a corresponding amount of M*n*-diol or NO*n*-diol (molar ratio 1:1.05) were weigh into a two-necked flask, mixed with a magnetic stirrer and heated to 160°C. Two drops of the catalyst Ti(IV) butoxide were added to the melted reactants. The reaction proceeded at 160°C under a nitrogen flow for 3 h, and at a reduced pressure (20 mbar) without nitrogen for another 3 h. After completion of the reaction, the cooled product mixture was dissolved in chloroform and precipitated with methanol. The reaction is depicted in scheme 2.

The polyesters are assigned according to the reagents as PIM6-M*n*, PIM6-NO*n*, PINO6-M*n* and PINO6-NO*n* (*n*=6, 8, 10, the number of CH_2 groups in the diol).

2.2. *Characterization*

^{1}H NMR spectra were recorded at 25°C on a Varian Unity Inova-300 spectrometer using $CDCl_3$ as the solvent and TMS as the internal standard. Average molar masses and molar mass distributions were determined relative to polystyrene standards by size exclusion chromatography (SEC) on a modular Perkin-Elmer liquid chromatograph equipped with a DAD detector working at a wavelength of 254 nm. A PL

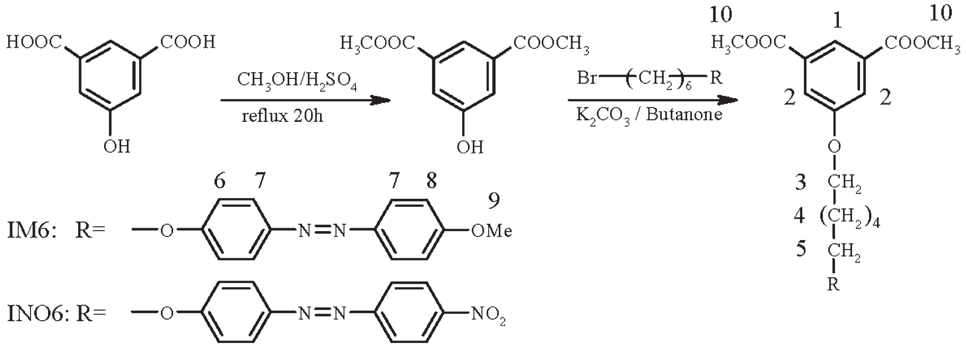

Scheme 1. The synthesis of IM6 and INO6.

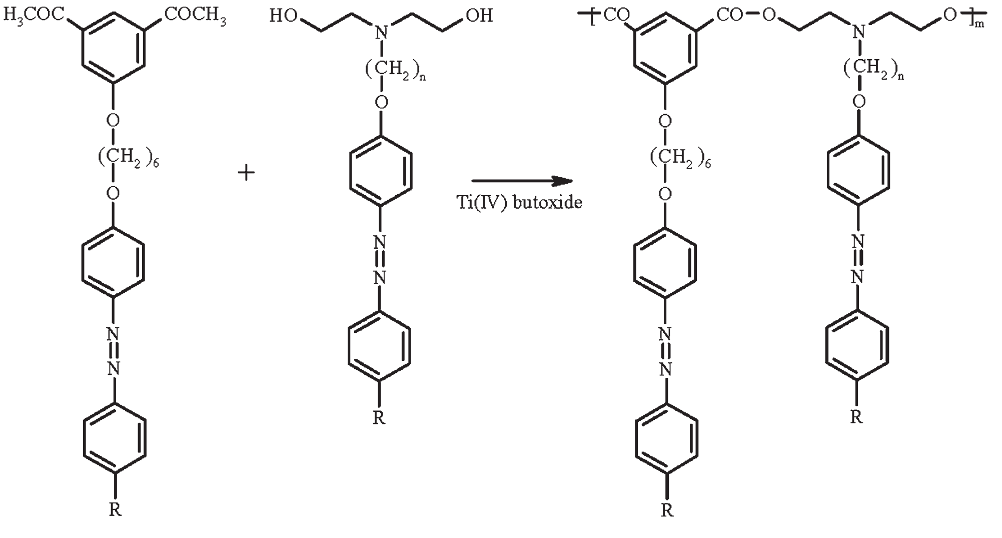

$R = OCH_3$ or NO_2, n = 6, 8, 10

Scheme 2. The synthesis of polyesters.

Mixed E column with a precolumn and THF as an eluant with a flow rate of $1\,\mathrm{ml\,min^{-1}}$ were used. DSC analysis was performed on a Perkin-Elmer Pyris 1 calorimeter. The samples were heated twice and subsequently cooled over a temperature range from $-10^{\circ}\mathrm{C}$ to $150^{\circ}\mathrm{C}$. Heating and cooling rates were $10\,\mathrm{K\,min^{-1}}$. Some polyesters were also tested at heating/cooling rates of 2 and $20\,\mathrm{K\,min^{-1}}$. Since there was no improvement in peak separation, only the results obtained at $10\,\mathrm{K\,min^{-1}}$ are present. XRD patterns were taken on a Siemens D-5000 diffractometer using Cu K_{α} radiation (λ=1.54Å) in 0.04° steps from 2–35° (in 2θ) with 2 s or 20 s per step. Optical textures were obtained using a Carl Zeiss polarizing optical microscope Stemi SV6 equipped with an MC 80 microscope camera and a Mettler Toledo FP82 hot stage.

3. Results and discussion

The yields of polyesters were 85–90%. The weight average molar masses were 4 000–8 000 $\mathrm{g\,mol^{-1}}$ and polydispersity indices were 2.0–2.9, which is similar to many other SC polyesters [12, 14, 19, 29]. ^{1}H NMR spectra confirmed the predicted structures of IM6, INO6, diols [17, 18], and polyesters. The proton signals are numbered as shown in scheme 1 and assigned as follows. IM6: 8.27 ppm (t, 1H, proton 1), 7.86 ppm (m, 4H, protons 7), 7.74 ppm (d, 2H, protons 2), 7.00 ppm (m, 4H, aromatic protons 6 and 8), 4.06 ppm (m, 4H, protons 3 and 5), 3.93 ppm (s, 6H, protons 10), 3.88 ppm (s, 3H, protons 9), 1.86 and 1.58 ppm (m, 4+4H, protons 4). INO6: 8.34 ppm (dt, 2H, protons 8), 8.25 ppm (t, 1H aromatic proton 1), 7.96 ppm (m, 4H, protons 7), 7.74 ppm (d, 2H, protons 2), 7.02 ppm (dt, 2H, protons 6), 4.06 ppm (m, 4H, protons 3 and 5), 3.93 ppm (s, 6H, protons 10), 3.88 ppm (s, 3H, protons 9), 1.86 and 1.58 ppm (m, 4+4H, protons 4).

In ^{1}H NMR spectra of polyesters signals are usually broad and many overlap with each other. Some triplets or doublets, which are formed due to long distance coupling (e.g. IM6: 8.27 or 7.74 ppm), are singlets in polyesters. A representative spectrum of PINO6-M6 is shown as an example in figure 1, where the diol signals are assigned as: 4.4 ppm ($-\mathrm{C\underline{H}_2}-\mathrm{O}-\mathrm{CO}-$), 3.6 ppm ($-\mathrm{C\underline{H}_2}-\mathrm{OH}$ end groups), 2.5–3 ppm ($-\mathrm{C\underline{H}_2}-\mathrm{N}-(\mathrm{C\underline{H}_2}-\mathrm{C\underline{H}_2})_2-$, small signals belonging to the end groups).

3.1. *Polyesters PIM6-Mn*

In the first heating scan the DSC curves of PIM6-M*n* exhibit several poorly separated endothermic peaks indicating crystalline structure. After a cooling and subsequent heating scan the DSC curves exhibit T_{g} and two peaks, which can be ascribed to crystal–liquid crystal (T_{m}, Cr–LC) and liquid crystal–isotropization (T_{i}, LC–I) transitions. Both transition temperatures increase with increasing side chain length, but the difference between the two transitions decreases. The glass transition temperature also increases with increasing side chain length (table 1). The DSC curves

Table 1. Thermal properties of PIM6-M*n* polyesters taken during the second heating scan.

Polyester	T_{g} °C	T_{m} °C	ΔH_{m} J g^{-1}	T_{i} °C	ΔH_{i} J g^{-1}
PIM6-M6	35.7	77.2	4.59	104.1	2.75
PIM6-M8	45.0	98.0	7.56	111.3	3.79
PIM6-M10	50.6	112.7	≈12.89	116.1	≈3.92

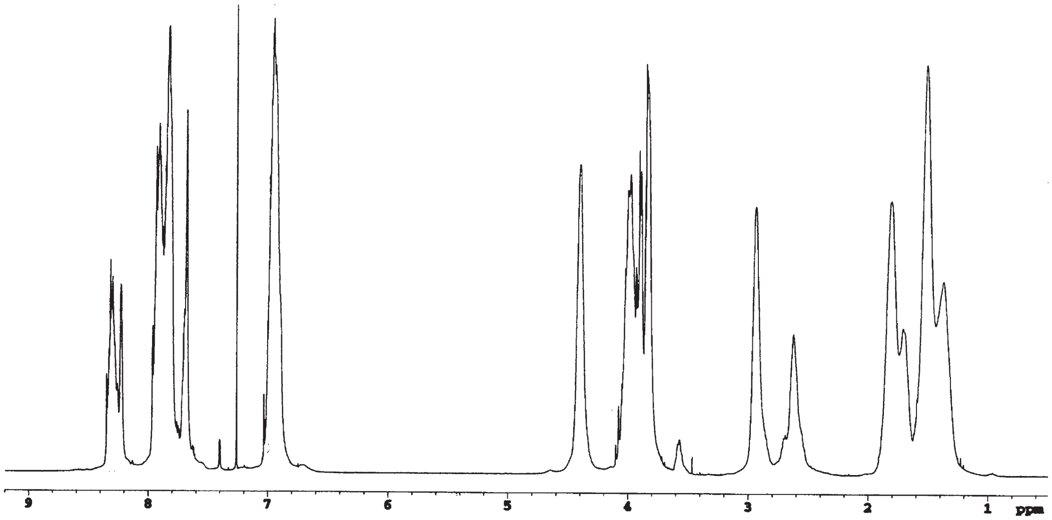

Figure 1. ^{1}H NMR spectra of polyester PINO6-M6.

of the second heating scan of PIM6-M*n* are shown in figure 2.

The existence of an LC phase was confirmed by POM and XRD. The X-ray diffractograms in the LC phase exhibit only one peak at $2\theta=21.5°$, indicating the formation of a nematic phase. The texture of the LC phase of PIM6-M6 at 100°C is shown as an example in figure 3.

3.2. *Polyesters PIM6-NOn*

The first heating DSC scan of PIM6-NO6 exhibits a weak glass transition and several endothermic peaks in the temperature range 40–110°C. PIM6-NO8 and PIM6-NO10 both exhibit a glass transition relaxation peak and one broad endothermic peak. After a cooling and subsequent heating scan all PIM6-NO*n* polyesters exhibit only one broad peak and the glass transition (table 2).

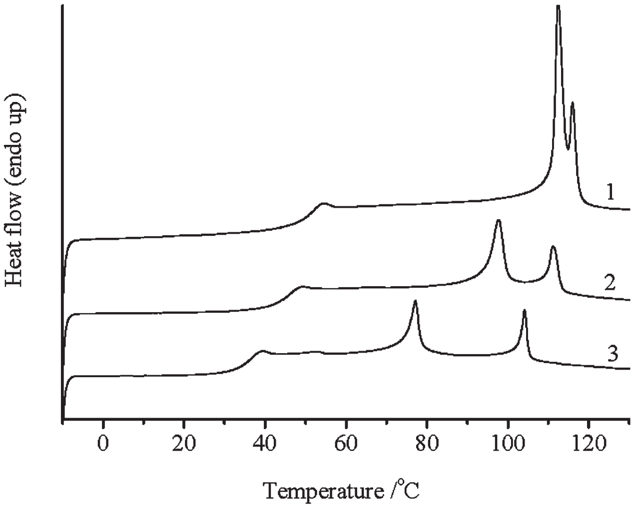

Figure 2. The second DSC heating curves of PIM6-M*n*: (1) PIM6-M10, (2) PIM6-M8, (3) PIM6-M6.

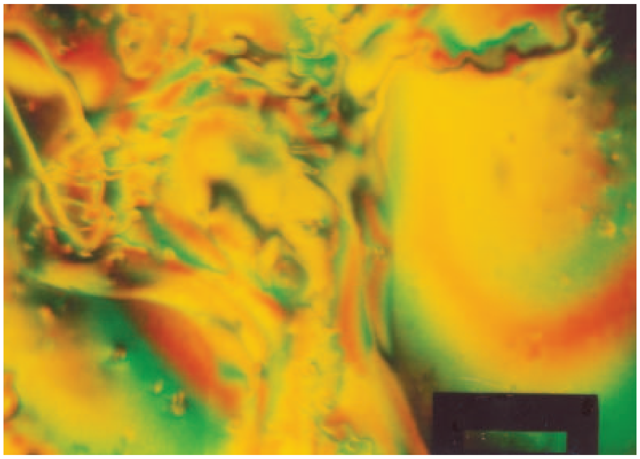

Figure 3. Texture of the nematic phase of PIM6-M6 taken at 100°C (magnification 125 X).

Thermal transitions observations on PIM6-NOn were followed by POM and XRD. PIM6-NO6 became a melt with sanded texture at 105°C. Isotropization started at 115°C but the last bright crystals disappeared at 155°C. The sanded texture appeared again on cooling at 107°C. There appear to be oligomers in the polyester, which melt at high temperatures. The X-ray diffractogram taken at room temperature confirms the crystalline structure of PIM6-NO6 (figure 4). There are several peaks between $2\theta=2°$ to 30° with the most intense peaks at 17° and 25°. At 110°C, when the polymer is melted (according to the DSC), the diffractions are much weaker, indicating a small quantity of crystalline material.

The melting of PIM6-NO8 as seen by POM started at 100°C; however, a melt of low viscosity having bright, sanded texture was formed at 120°C. At 130°C isotropization was observed, which is in agreement with the DSC curves; the sanded texture was formed on cooling at 119°C. In the diffractogram of PIM6-NO8,

Table 2. Thermal properties of PIM6-NO*n* polyesters taken during the second heating scan.

Polyester	T_g °C	T_m °C	ΔH_m J g^{-1}
PIM6-NO6	35.2	109.3	10.2
PIM6-NO8	37.3	115.7	10.4
PIM6-NO10	38.6	127.4	10.6

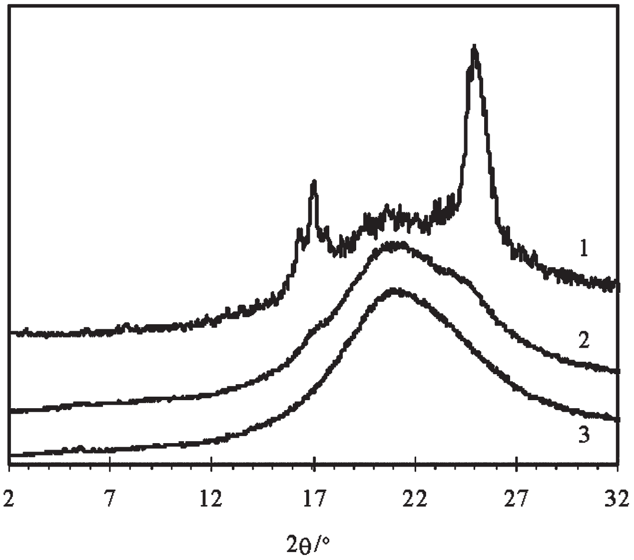

Figure 4. X-ray diffractograms: (1) PIM6-NO6, (2) PIM6-NO8, (3) PIM6-NO10.

taken at room temperature, only weak shoulders at 17° and 25° are observed in the main diffuse diffraction halo with an apex at 21°; these indicate the presence of a small fraction of crystalline phase in the polyester. At 100°C only a relatively sharp diffraction at 21° is present indicating the formation of a nematic phase.

The observations during heating of PIM6-NO10 under POM are similar to those for PIM6-NO6. Melting was observed at 120°C when the sanded texture was formed. The texture started turning to isotropic melt at 190°C; however, some small bright crystals were present in the isotropic melt up to 230°C. In the diffractogram of PIM6-NO10 taken at room temperature, there is a broad halo at 21° and only a very weak diffraction at 5.5°. According to the XRD the fraction of crystalline material seems to be very low.

On the basis of POM and X-ray diffractograms we cannot confirm or exclude liquid crystalline phases in PIM6-NO*n*. All the polyesters in the molten state exhibit sanded texture, which also appeared in the mixture of the isotropic melt of polyester and cyclic oligomers with a high melting point [21]. On the other hand, it is also possible that the polyesters are nematic but that the typical texture could not develop due to the presence of unmelted oligomers.

3.3. *Polyesters PINO6-Mn*

In the first heating scan the DSC curves of PINO6-M6 exhibit two overlapping peaks at 115 and 122.2°C. In the DSC curves of PINO6-M8 and PINO6-M10 there is only one broad peak for each, at 118.7 and 129.0°C, respectively. In the cooling curves of all three polyesters two peaks can be observed, although in the case of PIM6-M8 and the PIM6-M10 the peaks are strongly overlapping (figure 5). In the second heating scan (table 3) only one endothermic peak is observed, again for PIM6-M8 and PIM6-M10. In PIM6-M6 the temperature of the first transition was lowered to 113.5°C, while the second transition remained at 122.2°C. The heating curves are very similar to those shown later in Figure 7 and are therefore not presented. It seems that the smectic–nematic transition and isotropization are overlapping and as a consequence only one broad peak is observed for PINO6-M8 and PINO6-M10.

X-ray diffractograms of all PINO6-M*n* polyesters exhibit one or two weak diffractions in the low angle region and diffuse diffraction at $2\theta=21°$. In PINO6-M10 the diffractions in the low angle region are of the first (very weak) and second order indicating a liquid crystalline smectic phase with a layer thickness of 3.05 nm. Assuming that the only diffraction in the low angle region of the diffractograms of PINO6-M6 and PINO6-M8 is also of the second order, the layer thicknesses are 2.90 and 3.32 nm, respectively. It seems that for PINO6-M8, which has the thickest layer of the three polyesters, packing density is influenced by steric effects, which increases the thermal stability of its LC phase (table 3).

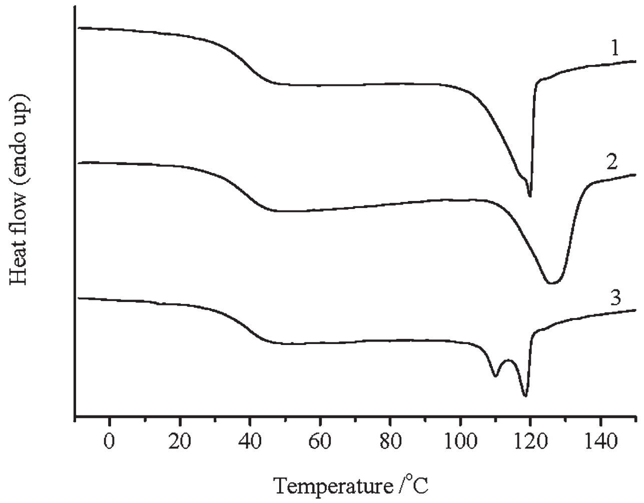

Figure 5. DSC cooling curves: (1) PINO6-M10, (2) PINO6-M8, (3) PINO6-M6.

The X-ray diffractogram of PINO6-M10 was recorded at 20 s per step in order to check the wide angle region, which is indicative of crystal or crystal smectic phases. No additional diffractions were observed meaning that these polyesters form an LC smectic phase (figure 6). The X-ray diffractogram of PINO6-M6 recorded at a temperature between the two endothermic transitions (117°C) exhibits only diffuse diffraction at 21°, indicating the formation of a nematic phase, which was also confirmed by POM. The free-flowing melt of PINO6-M6 was observed at 115°C and showed a marbled texture, which disappeared during the isotropization at 128°C.

On the basis of the DSC, XRD and POM results we can conclude that PINO6-M*n* polyesters form a liquid crystalline smectic phase, which on heating becomes a nematic phase. The type of smectic phase could not be

Table 3. Thermal properties of PINO6-M*n* polyesters taken during the second heating scan.

Polyester	T_g °C	T_i °C^a	ΔH_i J g^{-1a}
PINO6-M6	41.8	113.5, 122.2	4.2
PINO6-M8	39.4	128.0	9.3
PINO6-M10	40.4	118.2	9.3

[a] Due to the strong overlapping of the smectic–nematic transition and isotropization the results are presented as a single transition.

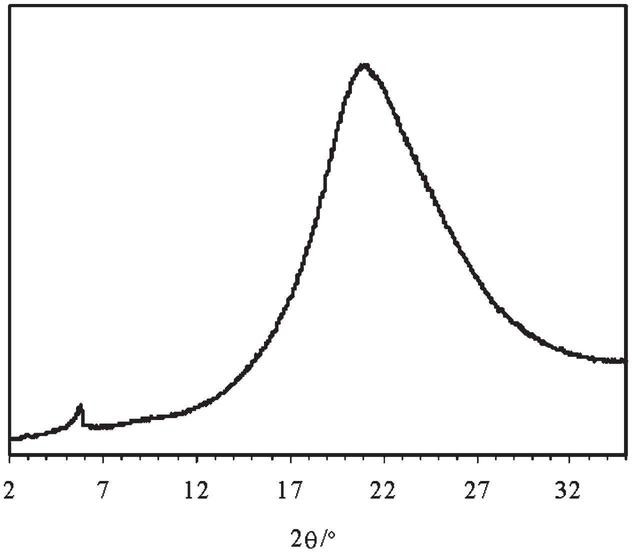

Figure 6. X-ray diffractogram of PINO6-M10.

determined on the basis of the powder diffraction spectra.

3.4. *Polyesters PINO6-NOn*

The DSC curves of PINO6-NO*n* are very similar to the DSC curves of PINO6-M*n* except that the transition temperatures are lower. The main difference is observed in the first heating scan where several small endothermic peaks were detected in PINO6-NO6 as well as in PINO6-NO10 at temperatures up to 105 and 120°C, respectively. The glass transition temperature of all the polyesters is in the range 31–36°C. In the second heating scan only one broad endothermic peak is observed for PINO6-NO8, while two overlapping peaks are observed for PINO6-NO6 and PINO6-NO10 (table 4). In PINO6-NO10 the gap between the peaks is very shallow so it appears as one flat peak (figure 7) The semi-crystalline structure of the polyesters was confirmed by XRD. The diffractogram of PINO6-NO6 is very similar to that of PINO6-M6 (figure 4). There are two relatively strong diffractions at $2\theta=17°$ and 25°, and one or several weak diffractions. The diffractions are much weaker in PINO6-NO10 and hardly visible in PINO6-NO8. When PINO6-NO10 was heated to 105°C there was only a diffuse diffraction at 21°; the formation of a liquid crystalline phase was confirmed by POM.

Table 4. Thermal properties of PINO6-NO*n* polyesters taken during the second heating scan.

Polyester	T_g °C	T_i °C[a]	ΔH_i J g^{-1}[a]
PINO6-NO6	31.0	81.0, 94.8	3.10
PINO6-NO8	35.5	114.2	2.84
PINO6-NO10	31.5	104.3, 106.5	4.70

[a] Due to the strong overlapping of melting and isotropization the results are presented as a single transition.

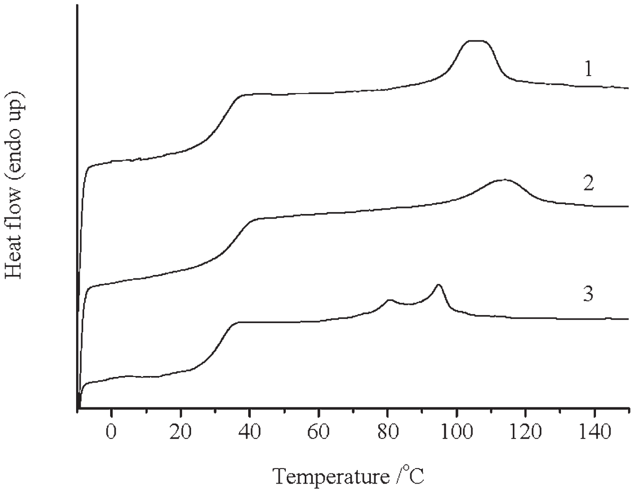

Figure 7. DSC curves of PINO6-NO*n* taken during the second heating scan: (1) PINO6-NO10, (2) PINO6-NO8, (3) PINO6-NO6.

When PINO6-NO6 was heated to 85°C (above the first transition peak) a marbled texture was formed, which turned into a homogeneous yellow texture upon further heating. The yellow texture disappeared during the isotropization at 110°C. By moving the cover glass at 112°C an LC phase was induced and the yellow texture reappeared (figure 8). The texture disappeared when stress was removed from the cover plate. The LC phase could be induced at temperatures up to 135°C. Similar behaviour was observed for PINO6-NO10. Above isotropization at 118°C, the nematic LC phase could be induced by moving the cover glass, up to

Figure 8. Induced LC phase of PINO6-NO6 at 112°C (magnification 125 X).

140°C. No induced LC phase was observed in PINO6-NO8. Since the molar mass of PINO6-NO8 ($4650\,\mathrm{g\,mol^{-1}}$) was between the molar masses of PINO6-NO6 ($3800\,\mathrm{g\,mol^{-1}}$) and PINO6-NO10 ($7900\,\mathrm{g\,mol^{-1}}$) this can only be explained by steric effects which could also lead to the T_m of PINO6-NO8 being higher than those of PINO6-NO6 and PINO6-NO10, similarly as it was observed and explained for PINO6-M*n* polyesters.

Flow-induced isotropic to nematic phase transitions have already been reported for acrylic SCLC polymers and main chain LC polyesters, but the temperature range was only up to 15°C above the isotropization temperature [22–24, 27], which is much less than in the described SCLC polyesters. According to the latest results the shear-induced transition is coupled with the existence of three-dimensional structure in the material and that the melt is not liquid but gel-like [28, 31].

3.5. *The influence of the type and position of the mesogenic group on the thermal properties of the polyesters*

The DSC curves of polyesters having a mesogenic unit bound to both the acid and the diol via a hexamethylene spacer are shown in figure 9. Although the polyesters differ only in the end groups of the side chains, they differ greatly in terms of thermal properties. It can be seen that the methoxy group increases T_g and isotropization temperatures when bound to the diol unit (compare curves 2 and 4 with 1 and 3, respectively) and decreases both when bound to an isophthalic acid residue (compare curves 3 and 4 with curves 1 and 2, respectively). The isotropization temperatures of polymers having both methoxy and nitro end groups are higher than those having only one type of end group, which is in agreement with the literature data and is ascribed to the interaction between the electron-rich and electron-deficient groups. This effect has already been observed in polyesters [14] as well as in some LC polymers based on methacrylates and 4-hydroxystyrene [32, 33].

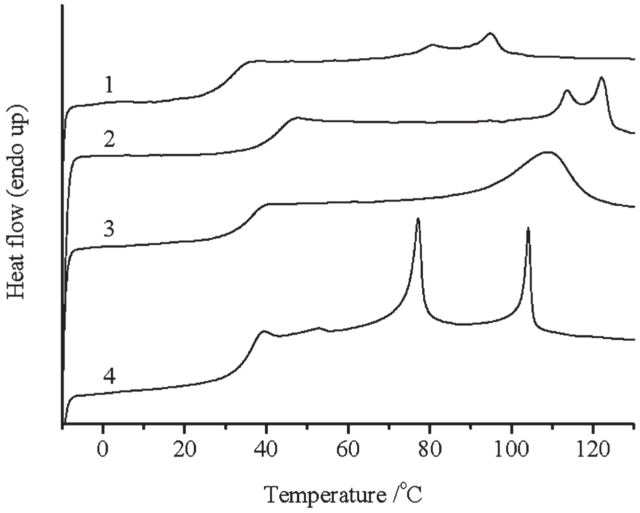

Figure 9. DSC curves of polyesters having the same spacer length in the diol and acid components: (1) PINO6-NO6, (2) PINO6-M6, (3) PIM6-NO6, (4) PIM6-M6.

4. Conclusions

We synthesized side chain polyesters having mesogenic methoxyazobenzene and/or nitroazobenzene groups bound to isophthalic acid as well as diethanolamine. The side chains were bound to the acid component via a spacer having six methylene units, while the length of the spacer between the diethanolamine and the mesogenic unit was 6, 8 or 10 methylene units. Depending on the type of mesogenic group on both the diethanolamine and isophthalic acid, four different types of polyesters were synthesized.

Most of the polyesters are crystalline at room temperature. According to the low melting enthalpies, relatively high ΔCp at the glass temperature (0.3–$0.5\,\mathrm{J\,g^{-1}\,K^{-1}}$), and X-ray diffractograms, we can conclude that the degree of crystallinity is low. The polyesters having a mesogenic group with a terminal –NO_2 group bound to isophthalic acid and a mesogenic group with a terminal –OCH_3 group bound to diethanolamine form a frozen liquid crystalline smectic phase at room temperature.

All polyesters were studied from an LC nematic phase on heating. The exception might be PIM6-NO*n* polyesters, where we were unable to confirm the presence of an LC phase.

The thermal properties of the polyesters depend on the type of mesogenic group, its position, and the length of the flexible spacer of the side chain. Their glass transition temperatures are in the range 30–50°C. A methoxy terminal group increases T_g and isotropization temperatures when bound to the diol and decreases both when bound to isophthalic acid. The length of the side chain has no specific effect on T_g, which has been observed not only in other polyesters [16], but also in LC polymers based on polystyrene having the same mesogenic groups as the synthesized polyesters [34].

Two of PINO6-NO*n* polyesters exhibit a rarely observed isotropic–nematic transition at temperatures more that 20°C above the isotropization temperature.

Acknowledgment

This research was supported by the Ministry of Higher Education, Science and Technology and Slovenian Research Agency (Program P2-0145).

References

[1] J.H. Wendorff, M. Eich. *Mol. Cryst. liq. Cryst.*, **169**, 133 (1989).
[2] U. Wiesner, N. Reynolds, C. Boeffel, H.W. Spies. *Makromol. Chem., rapid Commun.*, **12**, 457 (1991).
[3] J. Stumpe, L. Muller, D. Kreysig, G. Hauck, H.D. Koswig, R. Ruhmann, J. Rubner. *Makromol. Chem., rapid Commun.*, **12**, 81 (1991).
[4] T. Nakamura, T. Ueno, C. Tani. *Mol. Cryst. liq. Cryst.*, **169**, 167 (1989).
[5] C.S. Hsu. *Prog. polym. Sci.*, **22**, 829 (1997).
[6] L. Angiolini, L. Giorgini, R. Bozio, D. Pedron. *Synth. Met.*, **138**, 375 (2003).
[7] E. Ortyl, R. Janik, S. Kucharski. *Eur. polym J.*, **38**, 1871 (2002).
[8] H. Ringsdorf, C. Urban, W. Knoll, M. Savodny. *Makromol.Chem.*, **193**, 1235 (1992).
[9] D. Braun, R.P. Herr, N. Arnold. *Makromol. Chem. rapid Commun.*, **8**, 359 (1987).
[10] C.T. Imrie, B.J.A. Paterson. *Macromolecules*, **27**, 6673 (1994).
[11] J.V. Crivello, M. Deptolla, H. Ringsdorf. *Liq. Cryst.*, **3**, 235 (1988).
[12] T. Kodaira, M. Endo, M. Kurachi. *Macromol. Chem. Phys.*, **199**, 2329 (1998).
[13] C. Kulina, S. Hvilsted, C. Hendann, H.W. Siesler, P.S. Ramanujam. *Macromolecules*, **31**, 2141 (1998).
[14] B. Reck, H. Ringsdorf. *Liq. Cryst.*, **8**, 247 (1990).
[15] A. Böhme, E. Novotna, H. Kresse, F. Kuschel, J. Lindau. *Makromol. Chem.*, **194**, 3341 (1993).
[16] A. McRoberts, R. Denman, G.W. Gray, R.M. Scrowston. *Makromol.Chem., rapid Commun.*, **11**, 617 (1990).
[17] M. Brecl, T. Malavašič. *J.polym. Sci. A:polym. Chem.*, **35**, 2871 (1997).
[18] M. Brecl, M. Žigon. *Polymer*, **40**, 6529 (1999).
[19] M. Li, H. Qiu, X. Chen, E. Zhou, F. Jing. *Macromol. Chem. Phys.*, **200**, 834 (1999).
[20] M. Huskić, M. Žigon. *Polym. Bull.*, **53**, 35 (2004).
[21] M. Huskić, M. Žigon. *Polymer*, **44**, 6187 (2003).
[22] C. Pujolle-Robic, L. Noirez. *Nature*, **409**, 167 (2001).
[23] C. Pujolle-Robic, P.D. Olmsted, L. Noirez. *Europhys. Lett.*, **59**, 364 (2002).
[24] P.T. Mather, A. Romo-Uribe, C.D. Han, S.S. Kim. *Macromolecules*, **30**, 7977 (1997).
[25] N. Grizzuti, P.L. Maffettone. *J. chem. Phys.*, **118**, 5195 (2003).
[26] S. Hess, P. Ilg. *Rheologica Acta*, **44**, 465 (2005).
[27] P.T. Mather, H.G. Jeon, C.D. Han, S. Chang. *Macromolecules*, **35**, 1326 (2002).
[28] H. Mendil, P. Baroni, L. Noirez. *Europhysics. Lett.*, **72**, 983 (2005).
[29] N. Nemoto, F. Miyata, Y. Nagase, J. Abe, M. Hasegawa, Y. Shirai. *Macromolecules*, **29**, 2365 (1996).
[30] J.V. Crivello, M. Deptolla, H. Ringsdorf. *Liq. Cryst.*, **3**, 235 (1988).
[31] L. Noirez. *Phys. Rev.*, **E72**, 051701 (2005).
[32] C.T. Imrie, F.E. Karasz, G.S. Attard. *Liq. Cryst.*, **9**, 47 (1991).
[33] T. Schleeh, C.T. Imrie, D.M. Rice, F.E. Karasz, G.S. Attard. *J. polym. Sci. A: polym. Chem.*, **31**, 1859 (1993).
[34] C.T. Imrie, G.S. Attard, F.E. Karasz. *Macromolecules*, **29**, 1031 (1996).